ropolitan Police Hospital, Tokyo; Ideta Eye Hospital, Kumamoto; and Ehime University Hospital, Ehime, Japan. All of the subjects were enrolled from 2004 through 2010.

Routine ophthalmic examinations were performed on all patients. The criteria for classifying a patient as having POAG were: applanation IOP >22 mm Hg in each eye; glaucomatous cupping including cup-to-disc ratio >0.7 in each eye; visual field defects determined by Goldmann perimetry and/or Humphrey visual field analysis consistent with the glaucomatous cupping in at least 1 eye; and an open anterior chamber angle. Patients with glaucoma of secondary causes (eg, trauma-, uveitis-, or steroid-induced) were excluded. The criteria for NTG were applanation IOP <22 mm Hg in both eyes at each examination and the same characteristics as that of the POAG group. The IOP used for the statistical analyses was the clinic-based value. We checked the IOP in at least 3 visits and the measurements were made during the daylight hours. Patients were excluded if the IOP was 22 mm Hg or more for any of the measurements. The criteria for XFG were an open anterior chamber angle with accumulation of abnormal fibrillar material in the anterior segment of the eye and the same characteristics as the POAG group.

The control subjects (116 men and 100 women; age, 69.7 ± 11.3 years) had the following characteristics: IOP <22 mm Hg, normal optic discs, and no family history of glaucoma. To decrease the chance of studying individuals with presymptomatic glaucoma, we studied individuals who were older than 60 years in this group.

• SAMPLE PREPARATION AND MUTATION SCREENING: Genomic DNA was extracted from leukocytes of peripheral blood and purified with the Qiagen QIAamp DNA Blood Kit (Qiagen, Valencia, California, USA). Eight SNPs were amplified by polymerase chain reaction (PCR) using 0.5 μM intronic primers, 0.2 mM dNTPs, and 0.5 U Ex Taq polymerase (Takara, Shiga, Japan) with 30 ng template DNA in the amplification mixture (25 μL). The annealing temperature and sequence of primer set are given in the Supplemental Table (available at AJO.com).

Oligonucleotides for the amplification and sequencing were selected using Primer3 software (http://frodo.wi.mit.edu/cgi-bin/primer3/primer3_www.cgi/, provided in the public domain by the Massachusetts Institute of Technology, Cambridge, Massachusetts, USA). The PCR fragments were purified with ExoSAP-IT (USB, Cleveland, Ohio, USA), sequenced by the BigDye Terminator v3.1 Cycle Sequencing Kit (Perkin-Elmer, Foster City, California, USA) on an automated DNA sequencer (ABI PRISM 3100 Genetic Analyzer, Perkin-Elmer).

• STATISTICAL ANALYSES: Differences in the genotype frequencies among the cases and controls were tested by Fisher exact test or χ^2 depending on the cell counts. The inferred haplotypes and LD (linkage dysequilibrium), expressed as D',[23] quantified between all pairs of biallelic loci, were estimated using the SNPAlyze program version 5.0.3 (Dynacom, Yokohama, Japan). The significance of an association was determined by contingency table analysis using χ^2 or Fisher exact tests. The Hardy-Weinberg equilibrium was analyzed using gene frequencies obtained by simple gene counting and the χ^2 test with Yates' correction for comparing observed and expected values.

RESULTS

• HAPLOTYPE BLOCK: All of the 8 SNPs in the *TLR4* gene were genotyped, and all were in Hardy-Weinberg equilibrium in the glaucoma cases and control subjects. All SNPs were located in 1 haplotype block, and the magnitude of the LD between each SNP was very high, with a pairwise D' of more than 0.90. However, rs11536889 had a pairwise D' less than 0.80.

• ALLELE AND GENOTYPE FREQUENCIES IN *TLR4* VARIANTS DETECTED IN SUBJECTS: The allele frequencies of the 8 SNPs in the glaucoma cases and control subjects are shown in Table 1. The frequencies of the minor alleles of all SNPs were higher in the glaucoma cases than in control subjects. In the POAG subjects, the allele frequencies of 6 SNPs (rs10759930, rs1927914, rs1927911, rs12377632, rs2149356, and rs7037117) were significantly different from the control group ($P < .05$). In addition, 5 SNPs (rs10759930, rs1927914, rs1927911, rs2149356, and rs7037117) in NTG subjects and 4 SNPs (rs1927914, rs1927911, rs12377632, and rs2149356) in XFG subjects were significantly different from that in the control group ($P < .05$; Table 1). Three SNPs, rs1927914, rs1927911, and rs2149356, were identical for the POAG, NTG, and XFG groups. Among these 3 SNPs, the minor allele of rs2149356, located in intron 2 of *TLR4*, conferred the highest increased risk of POAG ($P = .000058$, OR = 1.77, 95% CI = 1.31–2.39), NTG ($P = .0030$, OR = 1.51, 95% CI = 1.17–1.95), and XFG ($P = .015$, OR = 1.56, 95% CI = 1.11–2.20).

The genotype frequencies of 8 SNPs are shown in Table 2. The genotype frequency of 5 SNPs was significantly higher in the POAG and NTG subjects than in the controls, and none of the SNPs was significantly higher in the XFG subjects than in the control group ($P = .16$, $P = .059$, $P = .080$, $P = .13$, $P = .062$, $P = .95$, $P = .12$, $P = .69$, respectively; χ^2 test). Considering the dominant model, 4 SNPs in the XFG group were significant compared with the genotype frequencies of the control group. In POAG, NTG and XFG individuals bearing the minor allele of rs2149356 had the most significantly increased risk for glaucoma over that of control subjects ($P = .00014$, $P = .015$, $P = .062$, respectively).

• HAPLOTYPE ANALYSIS: The haplotype frequencies of the Tag SNPs (rs10759930, rs11536889, rs7037117, and

TABLE 3. Haplotype Frequencies of Tag Single Nucleotide Polymorphisms of the Toll-like Receptor 4 Gene Compared with Previous Study

	This Study										Previous Study			
Tag SNPs rs10759930, rs11536889, rs7037117, and rs7045953	POAG (n = 184)	*P* Value	Overall *P* Value (POAG)	NTG (n = 365)	*P* Value	Overall *P* Value (NTG)	XFG (n = 109)	*P* Value	Overall *P* Value (XFG)	Control (n = 216)	NTG (n = 250)	Control (n=318)	*P* Value	Overall *P* Value (NTG)
TGAA	0.311	.000072	.00097	0.360	.003	.057	0.362	.036	0.134	0.448	0.350	0.402	.070	.044
TCAA	0.228	.882		0.242	.465		0.229	.863		0.223	0.226	0.247	.41	
CGAA	0.208	.030		0.164	.519		0.173	.439		0.150	0.166	0.159	.75	
CGGA	0.125	.406		0.137	.126		0.146	.141		0.107	0.154	0.102	.0090	
CGGG	0.090	.080		0.074	.280		0.067	.664		0.058	0.096	0.077	.26	
Tag SNPs rs10759930 and rs7037117														
TA	0.539	.00014	.0017	0.603	.020	.085	0.591	.044	0.201	0.674	0.575	0.649	.0044	.010
CG	0.216	.063		0.219	.023		0.219	.086		0.164	0.249	0.179	.21	
CA	0.238	.0073		0.178	.524		0.185	.479		0.162	0.173	0.169		

NTG = normal-tension glaucoma; POAG = primary open-angle glaucoma; SNP = single nucleotide polymorphism; XFG = exfoliation glaucoma.

TABLE 4. Haplotype Frequencies of Tag Single Nucleotide Polymorphisms of the Toll-like Receptor 4 Gene Between Primary Open-Angle, Normal-Tension, and Exfoliation Glaucoma and Control Subjects

Tag SNPs rs10759930, rs1927914, rs1927911, and rs2149356	POAG (n = 184)	*P* Value	Overall *P* (POAG)	NTG (n = 365)	*P* Value	Overall *P* (NTG)	XFG (n = 109)	*P* Value	Overall *P* (XFG)	Control (n = 216)
TTCC	0.516	.000014	.00078	0.589	.009	0.018	0.573	.020	.014	.667
CCTA	0.418	.00033		0.384	.003		0.395	.012		.296
CCCC	0.005	.138		0.008	.211		NA	NA		.016

NTG = normal-tension glaucoma; POAG = primary open-angle glaucoma; XFG = exfoliation glaucoma.

rs7045953) were studied earlier.[21] The results showed that NTG and XFG were not statistically significant (overall $P = .057$, $P = .134$), but POAG was statistically significant (overall $P = .00097$; Table 3). The tag SNPs, rs10759930 and rs7037117, used in that study were similar with these haplotypes (Table 3).

Other haplotypes, rs10759930, rs1927914, rs1927911, and rs2149356, had higher statistical significance (overall $P = .00078$ in POAG; overall $P = .018$ in NTG, and overall $P = .014$ in XFG; Table 4).

DISCUSSION

• TOLL-LIKE RECEPTOR 4 POLYMORPHISMS IN PRIMARY OPEN-ANGLE GLAUCOMA, NORMAL-TENSION GLAUCOMA, AND EXFOLIATION GLAUCOMA SUBJECTS: Shibuya and associates showed that rs7037117, located in the 3′-untranslated region of *TLR4*, was most strongly associated with NTG.[21] Compared to earlier reports, the intragenic SNP rs2149356 could be more associated with NTG and also with POAG and XFG in this study. The statistics of all 8 genotypes showed that *TLR4* had approximately the same tendency for all corresponded allele frequencies (Table 2). The haplotypes rs10759930, rs1927914, rs1927911, and rs2149356 had the higher statistically significant values in both groups (overall $P = .00078$, $P = .018$, and $P = .014$, respectively; Table 4). On the other hand, this haplotype was shown to be not significant, and even in the original study,[21] it was statistically marginal ($P = .044$ for 4 SNPs and $P = .010$ for 2 SNPs). Thus, these haplotypes and/or SNPs are valuable for screening for glaucoma in the Japanese.

Subjects enrolled in this study and those reported by Shibuya and associates[21] were from across Japan; however, the subjects from our study were predominantly from northern Japan. The difference in the heterogeneity may explain the slight differences between the 2 studies. An association between the SNPs and POAG and XFG was not expected before this study because the IOP has a predominant effect on these diseases. So it is interesting that *TLR4* would be associated with those phenotypes of POAG and XFG, and the risk associations were stronger in POAG than in NTG. Recently, Suh, and associates showed that *TLR4* gene polymorphisms do not associate significantly with NTG in a Korean population,[22] but they did not examine it in POAG and XFG subjects. It should be evaluated in various types of glaucoma in different populations.

• FUNCTION OF *TLR4* GENE: Innate immunity produces antimicrobial peptides against many kinds of pathogens in the host defense system, and these induce adaptive immunity secondarily. Together, they play important roles in the total immune system.[24] Targeting TLR signaling has implications in the control of infection, vaccine design, desensitization to allergens, and downregulation of inflammation. *TLR4*-deficient mice were reported to have an upregulation of NADPH oxidase (Nox3), which increased the oxidative stress.[25] Although the function of the 8 SNPs on the *TLR4* gene was not examined, rs10759930 and rs1927914 exist within the 5′ untranslated region, rs1927911, rs12377632, and rs2149356 exist within introns, and rs11536889, rs7037117, and rs7045953 exist within the 3′ untranslated region. There is a possibility that these SNPs influence the stability of the mRNA and expression of the *TLR4* gene because rs11536889 exists near exon3.

TLR4 is expressed in the conjunctiva, cornea, iris, ciliary body, choroid, retina, and retinal pigment epithelium. In the retina, changes in the glial cells may be associated with glaucoma, especially NTG, which is not so dependent on the IOP. Widespread chronic stress is evident in the retina and optic nerve head by the strong upregulation of the HSPs in glaucomatous eyes.[26] Recently, an upregulation of toll-like receptors TLR2, TLR3, and TLR4 was found in human glaucoma donor eyes, which is consistent with the strongly increased level of expression of HSPs.[27] Immunohistochemical analyses supported an upregulated expression of TLRs in both microglia and astrocytes in glaucomatous retinas. It has been postulated that changes in the microenvironment of injured axons will alter the glycosaminoglycan composition in the lamina cribrosa, and this may account for the increased vulnerability of the remaining axons to sustain further damage independent of the IOP.

The significance of these findings in POAG more than NTG raises further speculation. Chronic stress could influence the aqueous humor and may adversely affect the outflow structure to increase resistance to outflow, with alterations of the trabecular meshwork and intrascleral channels and collapse of the Schlemm canal. There is a possibility that *TLR4* might have an effect on the alterations of the aqueous humor dynamics and injury to the glaucomatous retina in eyes with POAG and XFG.

• AUTOIMMUNE DISEASES, CHRONIC INFLAMMATION, AND GLAUCOMA: To date, the genes of the TLR family have not been candidates as genetic modifiers of glaucoma susceptibility, but they have been implicated in other autoimmune diseases and allergic diseases, including rheumatoid arthritis[28,29] and bronchical asthma.[30,31] It is interesting that the net *TLR4* sequence variants and the *TLR4* signaling network would affect not only the development of NTG but also POAG and XFG. Chronic infection by certain bacteria and viruses may play a role in inflammation.[32] More specifically, chronic infection by *Helicobater pyori* may induce a persistent systemic and vascular inflammation and endothelial dysfunction.[33] The results of one study showed that the specific IgG antibody levels of *H. pylori* were significantly increased in the aqueous humor and serum of patients with POAG and

XFG.[34] In addition, the titer of *H. pylori* antibody in the aqueous humor might reflect the severity of glaucomatous damage in POAG patients. We hypothesized that some types of chronic infection and/or inflammation can lead to the development of glaucoma especially POAG.

In conclusion, we have identified *TLR4* SNPs as genetic susceptibility alleles for POAG, NTG, and XFG in the Japanese population. Our findings would support the idea that changes in the regulation of TLR signaling in human glaucoma may be associated with innate and adaptive immune responses. Further investigations on different ethnic populations, and on the structure and function of the *TLR4* protein, would be helpful in understanding the pathogenesis of POAG, NTG, and XFG.

ALL AUTHORS HAVE COMPLETED AND SUBMITTED THE ICMJE FORM FOR DISCLOSURE OF POTENTIAL CONFLICTS OF interest and none were reported. This study was supported in part by a Grant-In-Aid for Scientific Research from the Ministry of Education, Science, and Culture of the Japanese Government (NF; C-22591928), by grant from the Ministry of Health, Labor and Welfare of Japan to N.F., and by a grant from the Japan-China Medical Association, Japan, to D.S. Involved in conception and design of the study (Y.T., D.S., Y.M., N.F.); data collection (Y.T., D.S., Ai.S., To.F., N.Y., Ta.F., H.A., H.I., X.Z., At.S., Y.O., K.N.), analysis (Y.T., D.S., N.F.), and interpretation of data (T.Y., T.N., N.F.); and preparation, review, and approval of the manuscript (K.N., T.N., N.F.). The purpose and procedures of the experiment were explained to all patients, and informed consent was obtained. The procedures used conformed to the tenets of the Declaration of Helsinki, and this study was approved by the Tohoku University Institutional Review Board prospectively. Informed consent for participation in this research was obtained from all patients.

Y. Takano and D. Shi contributed equally to this work.

The authors thank Duco Hamasaki, Professor Emeritus, Bascom Palmer Eye Institute, University of Miami, Miami, Florida, for his critical comments and valuable assistance.

REFERENCES

1. Quigley H. Number of people with glaucoma worldwide. *Br J Ophthalmol* 1996;80(5):389–393.
2. Werner EB. Normal-tension glaucoma. In: Ritch R, Shields MB, Krupin T, eds. The Glaucomas, St. Louis: Mosby; 1996:769–797.
3. Shiose Y, Kitazawa Y, Tsukahara S, et al. Epidemiology of glaucoma in Japan—a nationwide glaucoma survey. *Jpn J Ophthalmol* 1991;35(2):133–155.
4. Iwase A, Suzuki Y, Araie M, et al. The prevalence of primary open-angle glaucoma in Japanese: the Tajimi Study. *Ophthalmology* 2004;111(9):1641–1648.
5. Shields MB. Molecular genetics and pharmacogenomics of the glaucomas. In: Shields MB, ed. Shields Textbook of Glaucoma, 6th ed. Baltimore (MD): Lippincott Williams & Wilkins; 2011:139–148.
6. Stone EM, Fingert JH, Alward WL, et al. Identification of a gene that causes primary open angle glaucoma. *Science* 1997;275(5300):668–670.
7. Rezaie T, Child A, Hitchings R, et al. Adult-onset primary open-angle glaucoma caused by mutations in optineurin. *Science* 2002;295(5557):1077–1079.
8. Monemi S, Spaeth G, DaSilva A, et al. Identification of a novel adult-onset primary open-angle glaucoma (POAG) gene on 5q22.1. *Hum Mol Genet* 2005;14(6):725–733.
9. Wiggs JL, Auguste J, Allingham RR, et al. Lack of association of mutations in optineurin with disease in patients with adult-onset primary open-angle glaucoma. *Arch Ophthalmol* 2003;121(8):1181–1183.
10. Hauser MA, Allingham RR, Linkroum K, et al. Distribution of WDR36 DNA sequence variants in patients with primary open-angle glaucoma. *Invest Ophthalmol Vis Sci* 2006;47(6):2542–2546.
11. Schlotzer-Schrehardt U, Naumann GO. Ocular and systemic pseudoexfoliation syndrome. *Am J Ophthalmol* 2006;141(5):921–937.
12. Thorleifsson G, Magnusson KP, Sulem P, et al. Common sequence variants in the LOXL1 gene confer susceptibility to exfoliation glaucoma. *Science* 2007;317(5843):1397–1400.
13. Hayashi H, Gotoh N, Ueda Y, Nakanishi H, Yoshimura N. Lysyl oxidase-like 1 polymorphisms and exfoliation syndrome in the Japanese population. *Am J Ophthalmol* 2008;145(3):582–585.
14. Fuse N, Miyazawa A, Nakazawa T, Mengkegale M, Otomo T, Nishida K. Evaluation of LOXL1 polymorphisms in eyes with exfoliation glaucoma in Japanese. *Mol Vis* 2008;14:1338–1343.
15. Ritch R. Exfoliation syndrome-the most common identifiable cause of open-angle glaucoma. *J Glaucoma* 1994;3(2):176–177.
16. Wax MB. Is there a role for the immune system in glaucomatous optic neuropathy? *Curr Opin Ophthalmol* 2000;11(2):145–150.
17. Wax MB, Tezel G, Saito I, et al. Anti-Ro/SS-A positivity and heat shock protein antibodies in patients with normal-pressure glaucoma. *Am J Ophthalmol* 1998;125(2):145–157.
18. Tezel G, Seigel GM, Wax MB. Autoantibodies to small heat shock proteins in glaucoma. *Invest Ophthalmol Vis Sci* 1998;39(12):2277–2287.
19. Park JS, Svetkauskaite D, He Q, et al. Involvement of toll-like receptors 2 and 4 in cellular activation by high mobility group box 1 protein. *J Biol Chem* 2004;279(9):7370–7377.
20. Akira S, Takeda K, Kaisho T. Toll-like receptors: critical proteins linking innate and acquired immunity. *Nat Immunol* 2001;2(8):675–680.
21. Shibuya E, Meguro A, Ota M, et al. Association of Toll-like receptor 4 gene polymorphisms with normal tension glaucoma. *Invest Ophthalmol Vis Sci* 2008;49(10):4453–4457.
22. Suh W, Kim S, Ki CS, Kee C. Toll-like receptor 4 gene polymorphisms do not associate with normal tension glaucoma in a Korean population. *Mol Vis* 2011;17:2343–2348.
23. Zhao JH, Curtis D, Sham PC. Model-free analysis and permutation tests for allelic associations. *Hum Hered* 2000;50:133–139.

24. Chaudhuri N, Dower SK, Whyte MK, Sabroe I. Toll-like receptors and chronic lung disease. *Clin Sci (Lond)* 2005; 109(2):125–133.
25. Zhang X, Shan P, Jiang G, Cohn L, Lee PJ. Toll-like receptor 4 deficiency causes pulmonary emphysema. *J Clin Invest* 2006;116(11):3050–3059.
26. Tezel G, Hernandez R, Wax MB. Immunostaining of heat shock proteins in the retina and optic nerve head of normal and glaucomatous eyes. *Arch Ophthalmol* 2000; 118(4):511–518.
27. Luo C, Yang X, Kain AD, Powell DW, Kuehn MH, Tezel G. Glaucomatous tissue stress and the regulation of immune response through glial Toll-like receptor signaling. *Invest Ophthalmol Vis Sci* 2010;51(11):5697–5707.
28. Radstake TR, Franke B, Hanssen S, et al. The Toll-like receptor 4 Asp299Gly functional variant is associated with decreased rheumatoid arthritis disease susceptibility but does not influence disease severity and/or outcome. *Arthritis Rheum* 2004;50(3):999–1001.
29. Kuuliala K, Orpana A, Leirisalo-Repo M, et al. Polymorphism at position +896 of the toll-like receptor 4 gene interferes with rapid response to treatment in rheumatoid arthritis. *Ann Rheum Dis* 2006;65(9):1241–1243.
30. Werner M, Topp R, Wimmer K, et al. TLR4 gene variants modify endotoxin effects on asthma. *J Allergy Clin Immunol* 2003;112(2):323–330.
31. Sackesen C, Karaaslan C, Keskin O, et al. The effect of polymorphisms at the CD14 promoter and the TLR4 gene on asthma phenotypes in Turkish children with asthma. *Allergy* 2005;60(12):1485–1492.
32. Danesh J, Collins R, Peto R. Chronic infections and coronary heart disease: is there a link? *Lancet* 1997;350(9075): 430–436.
33. Oshima T, Ozono R, Yano Y, et al. Association of Helicobacter pylori infection with systemic inflammation and endothelial dysfunction in healthy male subjects. *J Am Coll Cardiol* 2005;45(8):1219–1222.
34. Kountouras J, Mylopoulos N, Konstas AG, Zavos C, Chatzopoulos D, Boukla A. Increased levels of Helicobacter pylori IgG antibodies in aqueous humor of patients with primary open-angle and exfoliation glaucoma. *Graefes Arch Clin Exp Ophthalmol* 2003;241(11):884–890.

SUPPLEMENTAL TABLE. Primer Sequences for Toll-like Receptor 4 Gene Amplification Used in This Study

	Forward Primer	Reverse Primer	Annealing Temperature(C)
rs10759930	gtacagggtgtttgggagga	catggaccaatgctcttgtg	63
rs1927914	tgatgaggattgaaaatgtgga	acaaaatggtccctcacagc	60
rs1927911	ttaaatactccatatcattggggagac	gagagcattcagaaattagatgg	62
rs12377632	tggtatttggctttctgttcc	aaggtttctggggcaagttt	56
rs2149356	ccttggatcaagtttagccatt	tttccacaaaactcgctcct	60
rs11536889	ccctgtacccttctcactgc	gtttctgaggaggctggatg	62
rs7037117	ttaacccttcccacctttc	agagtttgggacctgctcaa	60
rs7045953	ttcccatgttccctcatttc	ggggcaaaagagaaactcct	59

Cell Mol Neurobiol (2012) 32:59–66
DOI 10.1007/s10571-011-9734-x

ORIGINAL RESEARCH

Regional Distribution and Cell Type-Specific Subcellular Localization of Prothymosin Alpha in Brain

Sebok Kumar Halder · Hiroshi Ueda

Received: 31 May 2011 / Accepted: 27 June 2011 / Published online: 13 July 2011

Abstract Prothymosin alpha (ProTα) is an acidic nuclear protein implicated in several cellular functions including cell survival. ProTα is found in the central nervous system, but the regional and cell type-specific expression patterns are not known. In this study, our immunohistochemical analysis demonstrated that ProTα is expressed ubiquitously throughout adult brain with difference in the intensity of region-specific protein reactivity. Interestingly, the highest ProTα signals were observed in the brain regions relevant to neurogenesis, such as sub-ventricular zone, granular cell layer of dentate gyrus, as well as granule cell layer of olfactory bulb. Strong immunoreactivity was also found in habenula, ependymal cells lining the dorsal third and fourth ventricle, and in neurons in the Purkinje cell layer of cerebellum. We showed that ProTα was strictly localized in the nuclei of neurons, while it was found in the cytosolic space of astroglial and microglial processes and cell body in the adult brain. To clarify the phenomenon underlying cytosolic localization of ProTα in non-neuronal cells, ZVAD-fmk, a caspase-3 inhibitor, was delivered intracerebroventricularly in the brain. At the follow-up 24 h after ZVAD-fmk injection, we found that nuclear intensity of ProTα was significantly increased in astrocytes, whereas the ProTα expression was not affected in microglia. The present study would contribute toward better understanding of physiological and pathophysiological roles of ProTα in the brain.

Keywords Subcellular localization · Neurogenesis · Caspase-3 · Habenula · Ependymal cell · Purkinje cell

S. K. Halder · H. Ueda (✉)
Division of Molecular Pharmacology and Neuroscience,
Nagasaki University Graduate School of Biomedical Sciences,
1-14 Bunkyo-machi, Nagasaki 852-8521, Japan
e-mail: ueda@nagasaki-u.ac.jp

Abbreviations

ProTα	Prothymosin alpha
SVZ	Sub-ventricular zone
LV	Lateral ventricle
3V	Third ventricle
4V	Fourth ventricle
CA	Cornu ammonis
Str rad	Stratum radiatum
DG	Dentate gyrus
GCL	Granular cell layer
i.c.v.	Intracerebroventricular
Z-VAD-fmk	Z-Val-Ala-Asp fluoromethyl ketone
DAB	3,3'-diaminobenzidine tetrahydrochloride
Amyg	Amygdala

Introduction

Prothymosin alpha (ProTα) is a small (12.6 kDa), nuclear protein that belongs to alpha-thymosin family, and widely distributed in variety of tissues, such as thymus, spleen, lung, kidney, liver, and brain (Haritos et al. 1984; Pineiro et al. 2000). ProTα, a signal peptide-deficient protein, is associated with cell functions, such as proliferation, division, and survival in various cells (Karapetian et al. 2005; Letsas and Frangou-Lazaridis 2006; Jiang et al. 2003; Gomez-Marquez 2007; Ueda 2008), and with genomic actions such as binding to linker histone H1, DNA packaging (Papamarcaki and Tsolas 1994; Diaz-Jullien et al. 1996; George and Brown 2010), chromatin remodeling (Gomez-Marquez 2007), and regulation of transcription (Martini et al. 2000); Karetsou et al. 2002). In addition to these intracellular functions, there are also several reports

about the immunoregulatory role of extracellular ProTα, such as activation of major histocompatibility complex (MHC) expression (Baxevanis et al. 1992), induction of antitumor and antiviral activity (Garbin et al. 1997; Mosoian et al. 2006), activation of immune cells, and cytokine production (Pineiro et al. 2000; Skopeliti et al. 2007). There is an interesting report that ProTα induces an immunosuppressive activity against viral infection through the activation of Toll-like receptor-4 (Mosoian et al. 2010). Although ProTα has been detected in mammalian tissues, very little is known about cellular and biological roles of ProTα in the nervous system. Recently, ProTα has been identified as a unique cell death regulatory molecule in that it converts the intractable cell death necrosis into the controllable apoptosis, which is in turn inhibited by brain-derived neurotrophic factor/BDNF (Ueda et al. 2007). In addition, the administration of ProTα also inhibited the cerebral and retinal ischemia-induced necrosis as well as apoptosis through up-regulation of BDNF or erythropoietin/EPO (Ueda 2009; Fujita et al. 2009; Ueda et al. 2010). The most recent investigation demonstrate that ProTα is localized in the nuclei of cultured cortical neurons and astrocytes (Matsunaga and Ueda 2010). However, the pattern of ProTα expression in cells in the central nervous system is yet unknown. In this study, we attempted to see the regional distribution and cell type-specific subcellular localization of ProTα in mouse brain.

Materials and Methods

Animals

Male MP-BL mice weighing 20–25 g were used for all the experiments. Mice were kept in a room maintained at constant temperature (21 ± 2°C) and relative humidity (55 ± 5%) with an automatic 12 h light/dark cycle with free access to standard laboratory diet and tap water. All the procedures were formally approved by Nagasaki University Animal Care Committee.

Drug Treatments

Z-Val-Ala-Asp fluoromethyl ketone (Z-VAD-fmk) was purchased from Sigma-Aldrich, St. Louis, USA. Z-VAD-fmk was dissolved in dimethyl sulfoxide (DMSO) and finally diluted in artificial cerebrospinal fluid (ACSF). Z-VAD-fmk was delivered intracerebroventricularly (i.c.v.) at a dose of 1 μg/5 μl in the mouse brain using Hamilton syringe. Control mice were treated with equal volume of ACSF in a same manner. Mice were sacrificed at 3 and 24 h after injection.

Tissue Preparations

Mice were deeply anesthetized with sodium pentobarbital (50 mg/kg) and perfused transcardially with 0.1 M potassium-free phosphate buffered saline (K^+-free PBS, pH 7.4) followed by 4% paraformaldehyde (PFA) in 0.1 M K^+-free PBS. Brain was then quickly removed and post-fixed in 4% PFA for 3 h, and immediately transferred to 25% sucrose solution (in 0.1 M K^+-free PBS) overnight for cryoprotection. Brain was frozen in cryoembedding compound, and the coronal brain sections were prepared at 30-μm thickness by cryostat for immunohistochemical analysis.

Characterization of Anti-ProTα Antibody

Anti-ProTα antibody (mouse monoclonal IgG 2F11; Enzo Life Sciences Int., PA, USA) recognizes *N*-terminal region of ProTα spanning amino acids 1–31. Immunohistochemical analysis was used for the characterization of anti-ProTα antibody against ProTα in mouse brain. The isolation and purification of recombinant ProTα used in this experiment were performed following the protocol as described previously (Fujita et al. 2009). To confirm that the immunoreactivity of ProTα is specific, another set of experiments using anti-ProTα IgG primary antibody pre-absorbed with purified mouse recombinant ProTα (rProTα) for 30 min (10:1 rProTα:anti-ProTα IgG [w/w]; antibody dilution 1:1,000 in 1% blocking buffer) was performed. Then, fluorescent immunostaining was performed by incubating brain coronal sections with preabsorbed anti-ProTα antibody. For control, brain sections were incubated with anti-ProTα IgG primary antibody (1:1,000; Enzo Life Sciences Int., PA, USA).

Immunohistochemical Analysis

To perform 3,3′-diaminobenzidine tetrahydrochloride (DAB) immunostaining, the floating coronal brain sections were incubated with 1% H_2O_2 solution for 30 min and washed with 0.1% Triton X-100 in phosphate-buffered saline (PBST). The sections were incubated with blocking buffer containing 2% BSA in PBST and goat antiserum to mouse IgG (1:50; Cappel laboratories, PA, USA). Sections were then incubated with anti-ProTα IgG primary antibodies (1:1,000; mouse monoclonal IgG 2F11; Enzo Life Sciences Int., PA, USA) in 1% blocking buffer overnight at 4°C. Then, the sections were incubated with biotin-conjugated secondary antibody (1:500; goat polyclonal anti-mouse IgG, Invitrogen, CA, USA) and subsequently treated with avidin–biotin peroxidase solution (ABC kit, Vectastain Vector, USA). ProTα reactivity was visualized by incubation with a solution containing 0.02% DAB (Dojindo,

Kumamoto, Japan), 0.005% H_2O_2 (WAKO, Japan) in 0.05 M Tris–HCl buffer (pH 7.6), 1% cobalt chloride ($CoCl_2$), and nickel sulfate 1% $NiSO_4$ solution (Sigma-Aldrich, St. Louis, USA). Coronal brain sections were dehydrated through a series of ethanol solutions, xylene, and cover-slipped with Permount (Fisher Scientific, Waltham, MA, USA). Immunoreactivity of ProTα-positive cells (black reaction products) was analyzed using BZ Image Measurement Software (Keyence, Tokyo, Japan). For fluorescence immunostaining, coronal brain sections were washed with K^+-free PBS and incubated with 50% methanol followed by 100% methanol for 10 min. Samples were pretreated with blocking buffer containing 2% BSA in 0.1% PBST and incubated overnight at 4°C with following primary antibodies: anti-MAP2 (1:500, rabbit polyclonal antibody, Chemicon, CA, USA); anti-GFAP (1:500, rabbit polyclonal antibody, Dako, Denmark); and anti-Iba1 (1:1,000, rabbit polyclonal antibody, WAKO, Japan); anti-ProTα IgG (1:1,000; mouse monoclonal IgG 2F11; Enzo Life Sciences Int., PA, USA). Brain sections were then incubated with FITC-conjugated Alexa Fluor 594-conjugated anti-rabbit IgG and Alexa Fluor 488-conjugated anti-mouse IgG secondary antibodies (1:300; Molecular Probes, CA, USA). The nuclei were visualized through Hoechst 33342 (1:10,000, Molecular Probes, CA, USA). Samples were then washed thoroughly with PBS, cover-slipped with Perma Fluor (Thermo Shandon, Pittsburgh, PA, USA), and examined under a confocal microscope imaging system (Axiovert 200 M, Scan module: LSM 5 PASCAL; Carl Zeiss MicroImaging, Inc.) with image browser software (Carl Zeiss MicroImaging, Inc.), and also with BZ Image Measurement Software (Keyence, Tokyo, Japan). For image preparation, immunohistochemical images were adjusted when necessary for contrast and brightness using Adobe Photoshop (San Jose, CA, USA).

Results

Regional Distribution of ProTα in Brain

The diaminobenzidine (DAB) immunohistochemical analysis using mouse brain coronal sections show that ProTα is expressed ubiquitously throughout the mouse brain (Fig. 1a–d). The strength of ProTα immunoreactivity was different in the several regions of hippocampus (Fig. 1e). Highly magnifying observation of hippocampal section revealed that the signals in the pyramidal neuronal cell layer of cornu ammonis (CA1-3) were stronger than in cells in the stratum radiatum and stratum oriens (Fig. 1f). Among the regions of hippocampus, the highest ProTα signals were observed in neurons of granular cell layer in dentate gyrus, the popular zone of neurogenesis (Fig. 1g).

Similar strong immunoreactivity was found in the subventricular zone (SVZ), few cells in the striatum close to SVZ (Fig. 1h), and in some cells in the granule cell layer (GC) of olfactory bulb (Fig. 1i). Stronger signals were also observed in the ependymal cell layer lining the lateral ventricle, a part of SVZ (Fig. 1h), and in the ependymal cell lining the fourth ventricle of cerebellum (Fig. 1j), whereas relatively weaker signals in peri-ventricular nucleus were observed in the hypothalamus (Fig. 1k).

In addition, we found strong signals in the choroids plexus (CP), ependymal cell layer lining the dorsal third ventricle (3DV), and habenula (Fig. 1l, m). Most interestingly, the strongest signals were observed in neurons in Purkinje cell layer in cerebellum (Fig. 1n).

Cell type-Specific Subcellular Localization of ProTα

To examine the cell type-specific expression of ProTα in mouse brain, fluorescent immunostaining of brain coronal sections was performed with antibodies against ProTα and specific cell markers, such as MAP2 for neurons, GFAP for astrocytes, and Iba-1 for microglia. Our triple immunostaining data revealed that ProTα was expressed and strictly localized in the nuclei of MAP2-positive neurons in CA1 pyramidal neuronal cell layer of hippocampus (Fig. 2a). On the other hand, ProTα immunoreactivity was also observed in both GFAP-positive astrocytes and Iba-1-positive microglia in the stratum radiatum of hippocampus (Fig. 2b, c, respectively). Interestingly, we found that ProTα signal was localized in both cytosolic space of astroglial and microglial processes and cell body in the adult brain. Similar expressions and subcellular localizations were observed in neurons (Fig. 3a, b), astrocytes (Fig. 3c, d) and microglia (Fig. 3e, f) in the striatum, and cortex of brain.

In order to make sure that the signal was specific for ProTα, antibody (mouse monoclonal anti-ProTα IgG, 2F11, Enzo Life Sciences Int., PA, USA) was pretreated with recombinant ProTα for 30 min, and subsequent immunostaining of brain coronal sections was performed. This antibody has been reported to bind to the N-terminal region of ProTα spanning amino acids 1–31. Our findings showed that the addition of recombinant ProTα in antibody completely abolished the ProTα signal in MAP-2-positive neurons (Fig. 2d), GFAP-positive astrocytes (Fig. 2e), and Iba-1-positive microglia (Fig. 2f).

Caspase-3 Inhibitor Redistributes ProTα in Astrocytes

Our previous study reported that caspase-3 activation cleaved off the nuclear localization signal of ProTα in astrocytes and released it from the nucleus (Matsunaga and Ueda 2010). In addition, as adult astrocytes are known to

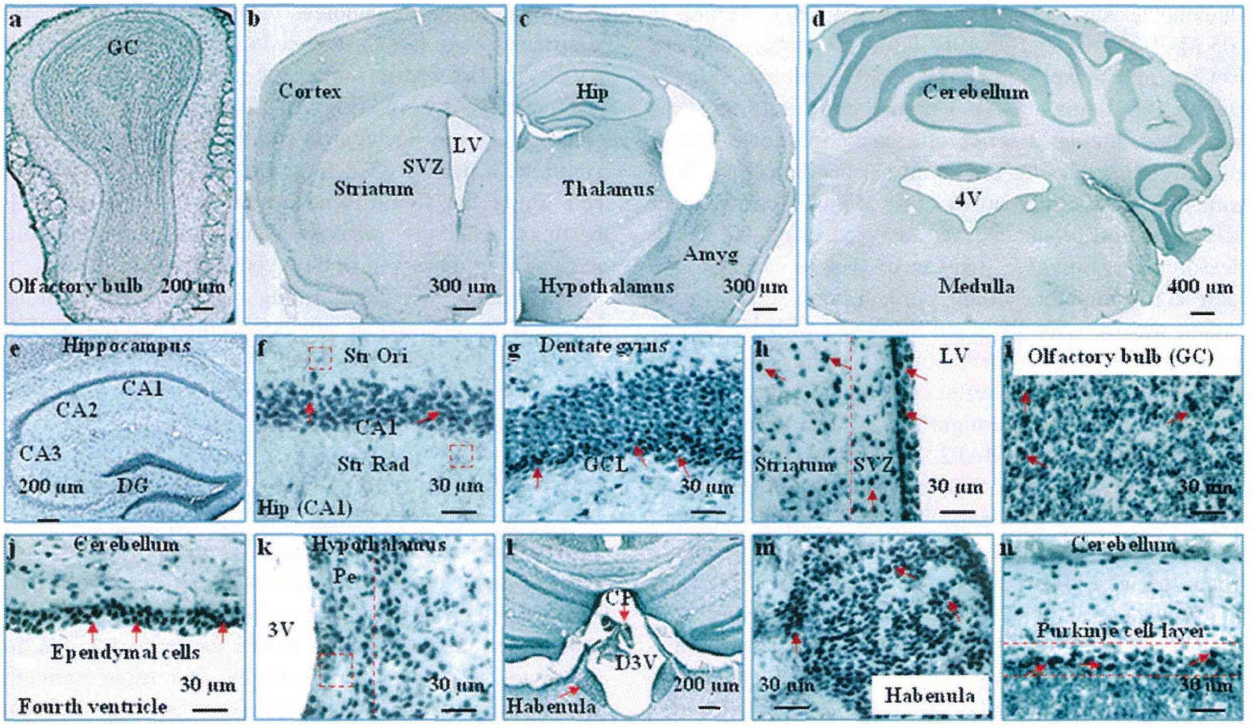

Fig. 1 Regional distribution of ProTα in the adult mouse brain. **a–n** DAB immunohistochemical analysis of coronal brain sections was performed, and ProTα immunoreactivity was observed using antibody against ProTα in brain. **a–d** Low magnification views of coronal sections show the general immunoreactivity of ProTα in the brain. DAB immunostaining data show the ProTα signals in the various regions of hippocampus (**e**) including cornu ammonis (CA1-3), stratum radiatum and stratum oriens (**f**) and dentate gyrus (**g**). ProTα signals are also found in sub-ventricular zone (SVZ) of the lateral ventricle (LV) and in some cells in the striatum close to the SVZ (**h**), granule cell layer (GC) of olfactory bulb (**i**), ependymal cell layer lining the fourth ventricle (**j**), periventricular nucleus (Pe) in hypothalamus (**k**), choroids plexus (CP) and ependymal cells lining dorsal third ventricle (**l**), habenula (**l**, **m**), and in purkinje cell layer in cerebellum (**n**). In figures **f–n**, the *arrowhead* points indicate the higher intensity of ProTα reactivity in brain. *Scale bars* **a**, **e**, **l** 200 μm, **b**, **c** 300 μm, **d** 400 μm, **f–k**, **m**, **n** 30 μm

have caspase-3 activity in the nucleus (Duran-Vilaregut et al. 2010); we attempted to see whether this protease inhibitor might redistribute ProTα. When Z-VAD-fmk, a caspase-3 inhibitor, was administered (i.c.v.) in brain and triple immunostaining performed at 3 and 24 h after injection, nuclear ProTα intensity was significantly increased in the nucleus of astrocytes in the stratum radiatum of hippocampus at 3 h (data are not shown) to 24 h (Fig. 4b), as compared to the control (Fig. 4a). On the other hand, no change in ProTα localization was observed in microglia at the same period after injection (Fig. 4c, d).

Discussion

In this study, we demonstrated that ProTα is expressed ubiquitously, but its regional expression varied throughout the adult mouse brain. Higher expression was found in dentate gyrus of hippocampus, SVZ of lateral ventricle and olfactory bulb, the regions which have been described as the popular areas for neurogenesis (Hack et al. 2005; Gould 2007; Zhao et al. 2008; Jin et al. 2010). ProTα expression was relatively higher in the granular cell layer (GCL) of dentate gyrus than the molecular layer. In the SVZ, more intense expression was found in the ependymal cell layer. It should be noted that some cells in the striatum close to the SVZ and in the granule cell layer of olfactory bulb also express intense signals. Taking it into consideration that GCL is the major locus for adult neurogenesis and newly born neurons in the adult SVZ migrate tangentially along the rostral migratory stream (RMS) to olfactory bulb (Brill et al. 2009) and also in the striatum (Ninomiya et al. 2006), it may be speculated that ProTα expression is related to the neurogenesis. However, ProTα expression is also high in the ependymal cells lining the fourth ventricle, where cerebrospinal fluid is produced, but little is known of the relationship of this region to neurogenesis. It is unlikely that the signals in ependymal cells at the edge of ventricle are caused by non-specific staining, since no prominent signals are found in the similar region at the third ventricle.

Higher expression was also observed in choroid plexus, habenula, and Purkinje cell layers of cerebellum. Choroid